DECOMPOSITION OF THE WAVE FIELD INTO OPTIMIZED GAUSSIAN PACKETS

K. ŽÁČEK

Department of Geophysics, Faculty of Mathematics and Physics, Charles University, Ke Karlovu 3, 121 16 Praha 2, Czech Republic (zacek@karel.troja.mff.cuni.cz, karelzacek@yahoo.com)

Received: October 28, 2005; Revised: March 7, 2006; Accepted: April 8, 2006

ABSTRACT

The decomposition of the wave field into optimized Gaussian packets represents a crucial step of the Gaussian packet prestack depth migration algorithm. The shape of optimized Gaussian packets, in the plane perpendicular to the central ray of the packet, depends not only on the frequency, but also on the coordinate of the intersection of the central ray of a Gaussian packet with the profile, on its arrival time, and on the component of the slowness vector along the profile. We express the amplitude of a Gaussian packet in the form of an integral transform similar to the forward coherent-state transform. Our method is suitable for a smooth distribution of the parameter determining the shape of a packet in the plane perpendicular to its central ray.

Key words: Gaussian packet, Gabor function, coherent-state transform, prestack depth migration, common shot gather

1. INTRODUCTION

Our long-term project is to explore the properties of a depth migration method based on Gaussian packets. Gaussian packets are waves whose envelopes at any given time are nearly Gaussian in space. They represent high-frequency asymptotic solutions of the elastodynamic equation, which are concentrated close to the central point of the packet (e.g., *Babich and Ulin, 1981*; *Ralston, 1983*; *Klimeš, 1989a, 2004*).

The main advantage of the Gaussian packet migration over the methods based on Gaussian beams is a direct relation between the regions in the common shot gather and corresponding localized regions in the migrated section.

Like Gaussian beams, Gaussian packets become inaccurate solutions of the elastodynamic equation if they spread excessively as they propagate. This spreading depends on the complexity of the velocity model and on the initial shape of Gaussian packets. Thus, we should use sufficiently smooth velocity model and optimize the initial shape of the packets.

The Gaussian packet migration algorithm consists of four basic steps:

a) Preparation of a suitable smooth velocity model (*Žáček, 2002*).

b) Optimization of the shape of Gaussian packets (*Klimeš, 1989b; Žáček, 2001, 2006*). Since narrow Gaussian packets quickly increase in width as they propagate, we can use neither too narrow nor too wide packets as the initial choice. In order to determine the optimum initial shape of Gaussian packets, we minimize the average squared widths of corresponding Gaussian beams and smooth the distribution of the optimum parameters of Gaussian beams on the Hamiltonian hypersurface in the phase-space.
c) Decomposition of the wave field into optimized Gaussian packets, which was already presented by *Žáček (2003)*, and which we thoroughly describe in this paper. The word optimized implies that such packets represent reasonably accurate solutions of the elastodynamic equation and that the shape of Gaussian packets, in the plane perpendicular to the central ray of the packet, depends not only on the frequency, but also on the coordinate of the intersection of the central ray of a Gaussian packet with the profile, on its arrival time, and on the component of the slowness vector along the profile.
d) Back propagation of the wave field using Gaussian packets and application of the imaging functional (*Žáček, 2004, 2005*). Each Gabor function from the common shot gather generates its localized image in the depth section. In this way, we obtain a one-to-one relation between the Gabor functions from the common shot gather and their localized images from the depth section.

The algorithm of the decomposition is designed here especially for numerical testing on the 2D Marmousi data set (*Versteeg and Grau, 1991*). That is why only 2D case is dealt with in this paper, although the generalization to 3D is straightforward.

2. DECOMPOSITION

We would like to approximate the wave field (common shot gather) $f(x,t)$ in the form of

$$\begin{aligned}\tilde{f}(x',t') = \int dt_R \int d\omega \exp\left[-\mathrm{i}\omega(t'-t_R)\right] \int dx_R \int dp \exp\left[-\mathrm{i}\omega p(x'-x_R)\right] \\ \times W(x'-x_R, t'-t_R, x_R, p, t_R, \omega) F(x_R, p, t_R, \omega),\end{aligned} \tag{1}$$

where x_R is the coordinate of the intersection of the central ray of a Gaussian packet with the profile, t_R denotes corresponding arrival time of a Gaussian packet, p is the component of the slowness vector a Gaussian packet along the profile, and ω is the positive circular frequency of a Gaussian packet. The complex-valued function W determines the shape of the envelope of a Gaussian packet, and the complex-valued function F specifies the amplitude of a Gaussian packet. Hereafter, the limits of integration with respect to x_R, t_R, x, t, and p are $-\infty$ and $+\infty$, and the limits of integration with respect to ω are 0 and $+\infty$.

Let us express the amplitude of a Gaussian packet in the form of an integral transform similar to the forward 2D coherent-state transform (e.g., *Klauder, 1987*; *Foster and Huang, 1991*; *Thomson, 2001*),

$$F\left(x_R,p,t_R,\omega\right)=\frac{\omega}{2\pi^2}\int dx\exp\left[-\mathrm{i}\omega p\left(x-x_R\right)\right]\int dt\exp\left[\mathrm{i}\omega\left(t-t_R\right)\right]\\ \times\omega\left(x_R-x,t_R-t,x_R,p,t_R,\omega\right)f\left(x,t\right), \tag{2}$$

where ω denotes a complex-valued analyzing function. Then, Eq.(1) can be expressed as

$$\widetilde{f}\left(x',t'\right)=\int dt\int d\omega\exp\left[\mathrm{i}\omega\left(t-t'\right)\right]\int dx\int dp\exp\left[-\mathrm{i}\omega p\left(x-x'\right)\right]\\ \times\frac{\omega}{2\pi^2}f\left(x,t\right)I\left(x'-x,t'-t,p,\omega\right), \tag{3}$$

where

$$I\left(x'-x,t'-t,p,\omega\right)\\ =\int dt_R\int dx_R\,W\left(x'-x_R,t'-t_R,x_R,p,t_R,\omega\right)w\left(x_R-x',t_R-t',x_R,p,t_R,\omega\right). \tag{4}$$

Considering convolution (4) independent of p, integration with respect to p in Eq.(3) yields a Dirac distribution $\delta\left(x'-x\right)$,

$$\widetilde{f}\left(x',t'\right)=\int dt\int d\omega\exp\left[\mathrm{i}\omega\left(t-t'\right)\right]\int dx\,\delta\left(x'-x\right)\frac{1}{\pi}f\left(x,t\right)I\left(x'-x,t'-t,0,\omega\right), \tag{5}$$

which can be integrated with respect to x,

$$\widetilde{f}\left(x',t'\right)=\int dt\int d\omega\exp\left[\mathrm{i}\omega\left(t-t'\right)\right]\frac{1}{\pi}f\left(x',t\right)I\left(0,t'-t,0,\omega\right). \tag{6}$$

Considering $I\left(0,t'-t,0,\omega\right)$ independent of ω, integration with respect to ω in Eq.(6) yields a complex-valued analytic Dirac distribution $\delta\left(t'-t\right)-\frac{\mathrm{i}}{\pi\left(t'-t\right)}$. Moreover, let us consider real-valued $I\left(0,t'-t,0,\omega\right)$, which leads to

$$\mathrm{Re}\left(\widetilde{f}\left(x',t'\right)\right)=\int dt\,\delta\left(t'-t\right)f\left(x',t\right)I\left(0,t'-t,0,\omega_0\right), \tag{7}$$

which can be integrated with respect to t,

$$\mathrm{Re}\left(\widetilde{f}\left(x',t'\right)\right)=f\left(x',t'\right)I\left(0,0,0,\omega_0\right). \tag{8}$$

For

$$I\left(0,0,0,\omega_0\right)=1, \tag{9}$$

the transformation would be exact,

$$\mathrm{Re}\left(\widetilde{f}\left(x,t\right)\right)=f\left(x,t\right). \tag{10}$$

The envelope of a trace of a Gaussian packet along the profile may be expressed as

$$W\left(x'-x_R,t'-t_R,x_R,p,t_R,\omega\right)=\exp\left[\mathrm{i}\omega\frac{1}{2}\left(\mathbf{y}'-\mathbf{y_R}\right)^T\mathbf{K}\left(\mathbf{y}'-\mathbf{y_R}\right)\right], \tag{11}$$

where

$$\mathbf{y}'=\begin{pmatrix}x'\\t'\end{pmatrix}, \tag{12}$$

$$\mathbf{y_R}=\begin{pmatrix}x_R\\t_R\end{pmatrix}, \tag{13}$$

and

$$\mathbf{K}=N\begin{pmatrix}1&0\\0&0\end{pmatrix}+N_{44}\begin{pmatrix}p^2&-p\\-p&1\end{pmatrix}. \tag{14}$$

Please note that parameters N and N_{44} correspond to N^0 and N_{44}^0, respectively, in *Žáček (2005, Eq.65)*.

Let us write the analyzing function w in an analogous form,

$$w\left(x'-x_R,t'-t_R,x_R,p,t_R,\omega\right)=\tilde{a}\exp\left[\mathrm{i}\omega\frac{1}{2}\left(\mathbf{y}-\mathbf{y_R}\right)^T\widetilde{\mathbf{K}}\left(\mathbf{y}-\mathbf{y_R}\right)\right], \tag{15}$$

where

$$\mathbf{y}=\begin{pmatrix}x\\t\end{pmatrix} \tag{16}$$

and

$$\widetilde{\mathbf{K}}=\widetilde{N}\begin{pmatrix}1&0\\0&0\end{pmatrix}+\widetilde{N}_{44}\begin{pmatrix}\tilde{p}^2&-\tilde{p}\\-\tilde{p}&1\end{pmatrix}. \tag{17}$$

The meaning and choice of parameters $\tilde{a}$, $\tilde{p}$, $\widetilde{N}$, and $\widetilde{N}_{44}$ is discussed below.

Neglecting the dependence of parameters N, N_{44}, $\tilde{a}$, $\tilde{p}$, $\widetilde{N}$, and $\widetilde{N}_{44}$ on x_R and t_R, we may calculate convolution (4),

$$I\left(x'-x,t'-t,p,\omega\right)$$
$$=\tilde{a}\int dt_R\int dx_R\exp\left[\mathrm{i}\omega\frac{1}{2}\left(\left(\mathbf{y}'-\mathbf{y_R}\right)^T\mathbf{K}\left(\mathbf{y}'-\mathbf{y_R}\right)+\left(\mathbf{y}-\mathbf{y_R}\right)^T\widetilde{\mathbf{K}}\left(\mathbf{y}-\mathbf{y_R}\right)\right)\right], \tag{18}$$

which leads to

$$I\left(x'-x,t'-t,p,\omega\right)$$
$$=\frac{2\pi\tilde{a}}{\omega\sqrt{\det\left[-\mathrm{i}\left(\mathbf{K}+\widetilde{\mathbf{K}}\right)\right]}}\exp\left[\mathrm{i}\omega\frac{1}{2}\left(\left(\mathbf{y}'-\mathbf{y}\right)^T\left(\mathbf{K}^{-1}+\widetilde{\mathbf{K}}^{-1}\right)^{-1}\left(\mathbf{y}'-\mathbf{y}\right)\right)\right]. \tag{19}$$

Inverse matrices to (14) and (17) read

$$\mathbf{K}^{-1}=\frac{1}{N_{44}}\begin{pmatrix}0&0\\0&1\end{pmatrix}+\frac{1}{N}\begin{pmatrix}1&p\\p&p^2\end{pmatrix} \tag{20}$$

and

$$\widetilde{\mathbf{K}}^{-1}=\frac{1}{\widetilde{N}_{44}}\begin{pmatrix}0&0\\0&1\end{pmatrix}+\frac{1}{\widetilde{N}}\begin{pmatrix}1&\tilde{p}\\\tilde{p}&\tilde{p}^2\end{pmatrix}. \tag{21}$$

In order to proceed from Eq.(3) to (5) and (6), we require $I\left(x'-x,t'-t,p,\omega\right)$ to be independent of p. Therefore, the sum $\mathbf{K}^{-1}+\widetilde{\mathbf{K}}^{-1}$ of matrices (20) and (21) in convolution (19) should be independent of p. To proceed from Eq.(6) to (7), we need $I\left(0,t'-t,0,\omega\right)$ to be independent of ω. This means that the rightmost diagonal component of matrix $\left(\mathbf{K}^{-1}+\widetilde{\mathbf{K}}^{-1}\right)^{-1}$ in convolution (19) should be proportional to ω^{-1}.

To meet these requirements, we choose the sum of matrices (20) and (21) in the form of

$$\mathbf{K}^{-1}+\widetilde{\mathbf{K}}^{-1}=\begin{pmatrix}2/N_0&0\\0&\dfrac{\omega}{K_0}+\dfrac{\omega}{\widetilde{K}_0}\end{pmatrix}, \tag{22}$$

where N_0, K_0, and $\widetilde{K}_0$ are constants. We introduce two generally different constants K_0 and $\widetilde{K}_0$, because we would like to choose $N_{44}=N_{44}\left(K_0\right)$ and $\widetilde{N}_{44}=\widetilde{N}_{44}\left(\widetilde{K}_0\right)$. Inserting expressions (20) and (21) into Eq.(22), we obtain three conditions,

$$\frac{1}{N}+\frac{1}{\widetilde{N}}=\frac{2}{N_0}\,, \tag{23}$$

$$\frac{p}{N}+\frac{\tilde{p}}{\widetilde{N}}=0 \tag{24}$$

and

$$\frac{p^2}{N}+\frac{1}{N_{44}}+\frac{\tilde{p}^2}{\widetilde{N}}+\frac{1}{\widetilde{N}_{44}}=\frac{\omega}{K_0}+\frac{\omega}{\widetilde{K}_0}\,, \tag{25}$$

where N_0, K_0, and $\widetilde{K}_0$ are free complex-valued constants that must be selected.

In 2D, the initial shape of a Gaussian packet is defined by two complex-valued parameters – N and K_0. The imaginary part of N determines the Gaussian packet width along the profile and the real part of N defines the curvature of the phasefront. We choose parameter K_0, which describes the shape of a Gaussian packet along the central ray, and which is connected with parameter N_{44} by Eq.(25), pure imaginary and uniform for all Gaussian packets.

In order to minimize the spreading of Gaussian packets, parameter N should be determined by the optimization of the shape of corresponding Gaussian beams (*Klimeš, 1989b; Žáček, 2001, 2006*). Consequently, we should consider optimized Gaussian packets,

$$N=N\left(x_R,t_R,p\right). \tag{26}$$

In this place, we must point out that the transformation is exact,

$$\widetilde{f}\left(x,t\right)-f\left(x,t\right), \tag{27}$$

only for N independent of x_R and t_R, see Eqs.(18) and (19). Nevertheless, for a reasonably smooth distribution of N with respect to x_R and t_R, we could achieve satisfactory results. Therefore, we have developed a procedure, which allows us to smooth iteratively the distribution of parameter N on a Hamiltonian hypersurface in the phase-space (*Žáček, 2001, 2006*).

Using Eqs.(23) and (24), we may write

$$\widetilde{N}=\frac{NN_0}{2N-N_0} \tag{28}$$

and

$$\tilde{p}=-\frac{\widetilde{N}}{N}\,p\,. \tag{29}$$

Please note that parameter p is real-valued, but $\tilde{p}$ is generally complex-valued.

Eq.(25) may be rearranged in several ways to determine parameters N_{44} and $\widetilde{N}_{44}$. For instance, we can get two symmetrical expressions,

$$\widetilde{N}_{44} = \frac{\widetilde{N}\widetilde{K}_0}{\omega\widetilde{N} - \tilde{p}^2\widetilde{K}_0} \tag{30}$$

and

$$N_{44} = \frac{NK_0}{\omega N - p^2 K_0}\,. \tag{31}$$

Then, pure imaginary constants $\widetilde{K}_0$ and K_0 must obey

$$\mathrm{Im}\left(\widetilde{K}_0\right) < \mathrm{Im}\left(\frac{\omega\widetilde{N}}{\tilde{p}^2}\right) \tag{32}$$

and

$$\mathrm{Im}\left(K_0\right) < \mathrm{Im}\left(\frac{\omega N}{p^2}\right). \tag{33}$$

Another approach would allow the use of the fast Fourier transform (FFT) in the decomposition (but not in the recomposition) of the wave field,

$$\widetilde{N}_{44} = \frac{\widetilde{K}_0}{\omega}, \tag{34}$$

$$N_{44} = \left(\frac{\omega}{K_0} - \frac{p^2}{N} - \frac{\tilde{p}^2}{\widetilde{N}}\right)^{-1}, \tag{35}$$

and

$$\mathrm{Im}\left(K_0\right) < \mathrm{Im}\left(\frac{\omega\left(2N - N_0\right)}{p^2}\right). \tag{36}$$

Eq.(9) requires

$$\tilde{a} = \frac{\omega}{2\pi}\sqrt{\det\left[-\mathrm{i}\left(\mathbf{K} + \widetilde{\mathbf{K}}\right)\right]}\,, \tag{37}$$

where matrix $\mathbf{K}$ is given by Eq.(14) and matrix $\widetilde{\mathbf{K}}$ by Eq.(17). Expression (37) with (14) and (17) can be converted using Eqs.(29) and (25) into

$$\tilde{a} = \frac{\omega}{2\pi}\sqrt{-\mathrm{i}\left(\mathbf{N} + \widetilde{\mathbf{N}}\right)}\sqrt{-\mathrm{i}N_{44}\widetilde{N}_{44}\left(\frac{\omega}{K_0} + \frac{\omega}{\widetilde{K}_0}\right)}\,, \tag{38}$$

where the square roots should be taken with positive real parts.

3. DISCRETIZATION

A proper choice of the discretization of integral (1) is not only of key importance in the decomposition of the wave field into Gaussian packets, but it also affects the accuracy and efficiency of the Gaussian packet migration.

Let us consider a 2D integral

$$\int d\xi_1 \int d\xi_2 \exp\left(\mathrm{i}\xi_J D_{JK} \xi_K\right) \tag{39}$$

discretized on a regular rectangular grid with intervals $\Delta\xi_1$ and $\Delta\xi_2$. Sufficient conditions for the discretization were derived by *Klimeš (1986)*,

$$\Delta\xi_1 \le \kappa \sqrt{-\left[\mathrm{Im}\left(\mathbf{D}^{-1}\right)\right]_{11}} \tag{40}$$

and

$$\Delta\xi_2 \le \kappa \sqrt{-\left[\mathrm{Im}\left(\mathbf{D}^{-1}\right)\right]_{22}} \,. \tag{41}$$

Matrix **D** must satisfy

$$\left|\left[\mathrm{Im}\left(\mathbf{D}^{-1}\right)\right]_{12}\right| \le \frac{1}{2}\sqrt{\left[\mathrm{Im}\left(\mathbf{D}^{-1}\right)\right]_{11}\left[\mathrm{Im}\left(\mathbf{D}^{-1}\right)\right]_{22}} \,. \tag{42}$$

The error of discretization depends on the properties of the wave field. For a simple wave field with linear amplitudes and quadratic arrival times, the relative maximum discretization error is about

$$\delta_{MAX} = 4\exp\left(-\pi^2\kappa^{-2}\right). \tag{43}$$

Then, the maximum relative error for $\kappa^2 = \pi/2$ would be about 0.7%. Unfortunately, the error may raise rapidly for a more complex wave field. In the worst case, the maximum relative error could reach up to 21% for $\kappa^2 = \pi/2$, see Table 3.3 in *Daubechies (1992)*. Nevertheless, we believe that a reasonable value of κ for a realistic wave field would be close to $\kappa^2 = \pi/2$.

The error of discretization of integral (18) with respect to x_R and t_R is controlled by matrix

$$\mathbf{D} = \frac{1}{2}\omega\left(\mathbf{K} + \widetilde{\mathbf{K}}\right). \tag{44}$$

According to conditions (40) and (41), maximum step in x_R for replacement of integral (18) by its discretized counterpart is

$$\Delta x_R = \kappa \sqrt{-\frac{2}{\omega}\left[\mathrm{Im}\left(\left(\mathbf{K} + \widetilde{\mathbf{K}}\right)^{-1}\right)\right]_{11}} \,, \tag{45}$$

maximum step in t_R is

$$\Delta t_R = \kappa \sqrt{-\frac{2}{\omega}\left[\mathrm{Im}\left(\left(\mathbf{K}+\widetilde{\mathbf{K}}\right)^{-1}\right)\right]_{22}}\,, \tag{46}$$

and we require

$$\left|\left[\mathrm{Im}\left(\left(\mathbf{K}+\widetilde{\mathbf{K}}\right)^{-1}\right)\right]_{12}\right| \le \frac{1}{2}\sqrt{\left[\mathrm{Im}\left(\left(\mathbf{K}+\widetilde{\mathbf{K}}\right)^{-1}\right)\right]_{11}\left[\mathrm{Im}\left(\left(\mathbf{K}+\widetilde{\mathbf{K}}\right)^{-1}\right)\right]_{22}}\,. \tag{47}$$

Eq.(3) can be understood as a convolution of functions

$$J\left(x,t,p,\omega\right) = \frac{\omega}{2\pi^2} I\left(x,t,p,\omega\right)\exp\left(\mathrm{i}\omega p x\right)\exp\left(-\mathrm{i}\omega t\right) \tag{48}$$

and $f(x, \mathrm{t})$ with respect to x and t, integrated over p and ω. Fourier transform $\widetilde{f}\left(k',\omega'\right)$ of $\widetilde{f}\left(x',t'\right)$ is then the product of Fourier transforms $J\left(k',\omega',p,\omega\right)$ and $f\left(k',\omega'\right)$, integrated over p and ω. Inserting convolution (19) into (48) and using the Fourier transform, we obtain $J\left(k',\omega',p,\omega\right)$ in the form similar to integral (39) with $\xi_1 = k'$ and $\xi_2 = \omega'$. The error of discretization of the integral of $J\left(k',\omega',p,\omega\right)$ with respect to $k = \omega p$ and ω is then controlled by matrix

$$\mathbf{D} = -\frac{1}{2}\omega^{-1}\left(\mathbf{K}^{-1}+\widetilde{\mathbf{K}}^{-1}\right). \tag{49}$$

According to conditions (40) and (41), maximum step in p is

$$\Delta p = \kappa \sqrt{\frac{2}{\omega}\left[\mathrm{Im}\left(\left(\mathbf{K}^{-1}+\widetilde{\mathbf{K}}^{-1}\right)^{-1}\right)\right]_{11}}\,, \tag{50}$$

maximum step in ω is

$$\Delta \omega = \kappa \sqrt{2\omega\left[\mathrm{Im}\left(\left(\mathbf{K}^{-1}+\widetilde{\mathbf{K}}^{-1}\right)^{-1}\right)\right]_{22}}\,, \tag{51}$$

and we require

$$\begin{aligned}&\left|\left[\mathrm{Im}\left(\left(\mathbf{K}^{-1}+\widetilde{\mathbf{K}}^{-1}\right)^{-1}\right)\right]_{12}\right| \\ &\le \frac{1}{2}\sqrt{\left[\mathrm{Im}\left(\left(\mathbf{K}^{-1}+\widetilde{\mathbf{K}}^{-1}\right)^{-1}\right)\right]_{11}\left[\mathrm{Im}\left(\left(\mathbf{K}^{-1}+\widetilde{\mathbf{K}}^{-1}\right)^{-1}\right)\right]_{22}}\,.\end{aligned} \tag{52}$$

Using conditions (23–25), we can simplify expressions (50) and (51) into

$$\Delta p = \kappa \sqrt{\frac{\mathrm{Im}\left(N_0\right)}{\omega}} \tag{53}$$

and

$$\Delta\omega = \kappa\sqrt{2\,\mathrm{Im}\left(\frac{K_0\widetilde{K}_0}{K_0+\widetilde{K}_0}\right)}\,. \tag{54}$$

Presented discretization conditions are valid for a general smooth distribution of parameter N on a Hamiltonian hypersurface in the phase-space, see Eq.(26). However, to simplify the whole migration procedure, it might be useful to smooth the optimized distribution of parameter N to a constant value as described by *Žáček (2001, 2006)*. Considering uniform Gaussian packets with $N = \widetilde{N} = N_0$, $K_0 = \widetilde{K}_0$, $\widetilde{N}_{44}$ given by Eq.(30) and N_{44} determined by Eq.(31), maximum discretization steps according to Eqs.(45), (46), (53), and (54) read

$$\Delta x_R = \frac{\kappa}{\omega}\sqrt{-\mathrm{Im}\left[\left(\omega N_0 - p^2 K_0\right)N_0^{-2}\right]}\,, \tag{55}$$

$$\Delta t_R = \kappa\sqrt{-\mathrm{Im}\left[\left(\omega N_0 - p^2 K_0\right)N_0^{-1}K_0^{-1}\right]}\,, \tag{56}$$

$$\Delta p = \kappa\sqrt{\frac{\mathrm{Im}\left(N_0\right)}{\omega}}\,, \tag{57}$$

and

$$\Delta\omega = \kappa\sqrt{\mathrm{Im}\left(K_0\right)}\,. \tag{58}$$

Naturally, uniform Gaussian packets bring about more rapid spreading, which could jeopardize the accuracy of the migration.

4. NUMERICAL EXAMPLES

We tested our method on a common shot gather belonging to the Marmousi data set (*Versteeg and Grau, 1991*), see Fig. 1. We decomposed the gather $f(x, t)$ using Eq.(2) into individual Gabor functions, see Fig. 2. The complex-valued amplitude of a Gaussian packet equals the amplitude of the corresponding Gabor function.

In order to examine the accuracy of our method, we composed the approximated common shot gathers $\widetilde{f}\left(x,t\right)$ according to Eq.(1), see Fig. 3. The differences between the original gather and the approximated gathers are shown in Fig. 4. We calculated all the numerical examples with $\kappa^2 = \pi/2$.

In the first example, we present the decomposition of the wave field into uniform Gaussian packets with $\mathrm{Re}(N_0) = 0.25 \times 10^{-6}$ sm^{-2} and $\mathrm{Im}(N_0) = 0.25 \times 10^{-6}$ sm^{-2}. See Fig. 3a for the corresponding approximated common shot gather. Fig. 4a indicates that the transformation is almost exact.

The next example demonstrates the decomposition of the wave field into Gaussian packets with varying parameter N. In this case, $\mathrm{Re}(N) = 0.25 \times 10^{-6}$ sm^{-2} and $\mathrm{Im}(N)$ ranges from 0.125×10^{-6} sm^{-2} to 0.5×10^{-6} sm^{-2}, which means that the widest Gabor function is, for a given frequency, two times wider then the narrowest one. The approximated gather is in Fig. 3b. According to Fig. 4b, the differences between the

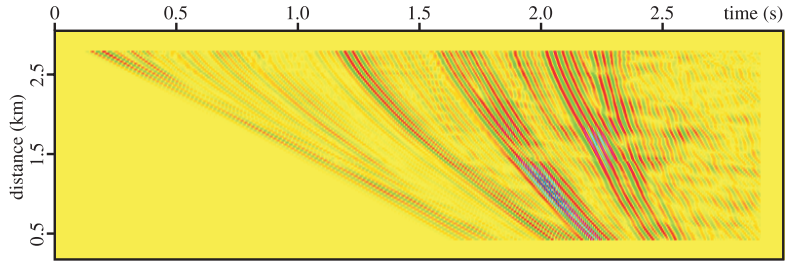

Fig. 1. Original common shot gather $f(x, t)$ of the Marmousi data set (*Versteeg and Grau, 1991*).

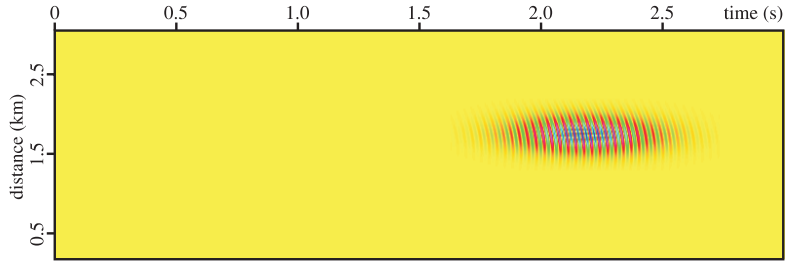

Fig. 2. Gabor function.

original and the approximated wave field can be spotted not only at the edges of the gather. This is caused by the dependency of parameter N on x_R and t_R.

The last example is the decomposition of the wave field with $\mathrm{Re}(N) = 0.25 \times 10^{-6}$ sm^{-2} and $\mathrm{Im}(N)$ varying from 0.75×10^{-7} sm^{-2} to 0.1×10^{-5} sm^{-2}, which means that the widest Gabor function is, for a given frequency, 3.6 times wider then the narrowest one. The approximated gather is displayed in Fig. 3c. Although we can note several differences between the original and the approximated gather in Fig. 4c, the result seems to be satisfactory.

The only serious problem of our method is the computational cost, because we cannot use 2D FFT. The mathematical formulation of our task allows only a series of 1D FFTs in the decomposition, but not in the recomposition of the wave field. In order to make the decomposition of the wave field more efficient, we are constantly trying to refine the algorithm and speed up the computations.

5. CONCLUSIONS

The presented procedure of the decomposition of the wave field into Gaussian packets is fully functional. It might be suitable not only for Gaussian packet migration, but also for many different applications of the Gaussian packet method.

The choice of the discretization of the integral transform plays a crucial role in the decomposition of the wave field. It affects not only the accuracy, but also the efficiency of

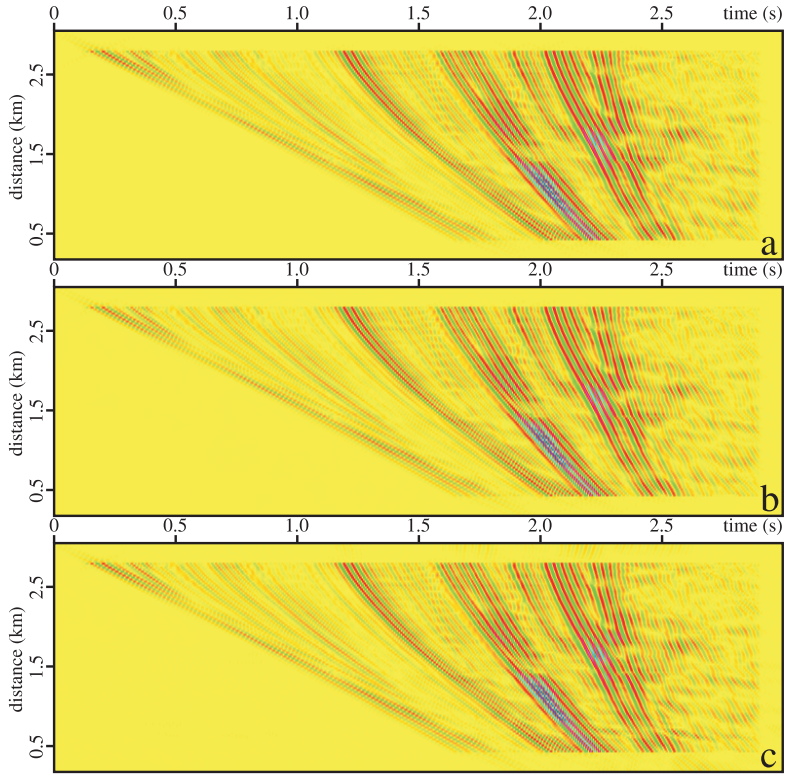

Fig. 3. Approximated common shot gathers $\tilde{f}(x,t)$ for **(a)** uniform Gaussian packets with $\mathrm{Re}(N_0) = 0.25 \times 10^{-6}$ sm^{-2} and $\mathrm{Im}(N_0) = 0.25 \times 10^{-6}$ sm^{-2}; **(b)** Gaussian packets with $\mathrm{Re}(N) = 0.25 \times 10^{-6}$ sm^{-2} and $\mathrm{Im}(N)$ ranging from 0.125×10^{-6} sm^{-2} to 0.5×10^{-6} sm^{-2}; **(c)** Gaussian packets with $\mathrm{Re}(N) = 0.25 \times 10^{-6}$ sm^{-2} and $\mathrm{Im}(N)$ ranging from 0.75×10^{-7} sm^{-2} to 0.1×10^{-5} sm^{-2}.

the method. We are able to control the discretization error of the decomposition into uniform Gaussian packets.

Decomposition of the wave field into Gaussian packets, whose shape depends on the coordinate of the intersection of the central ray of a Gaussian packet with the profile and on its arrival time, is, strictly mathematically speaking, incorrect. In order to achieve satisfactory results even in such a case, we smooth the distribution of the parameter determining the shape of a packet in the plane perpendicular to its central ray (*Žáček, 2001, 2006*).

Naturally, the price we have to pay for a smooth distribution of the initial parameters of Gaussian packets is a faster spreading of packets, which may lead, in a complex structure, to an inaccurate solution of the elastodynamic equation. In other words, we have to deal with a trade-off between the accuracy of the decomposition of the wave field and the accuracy of the Gaussian packet solution of the elastodynamic equation.

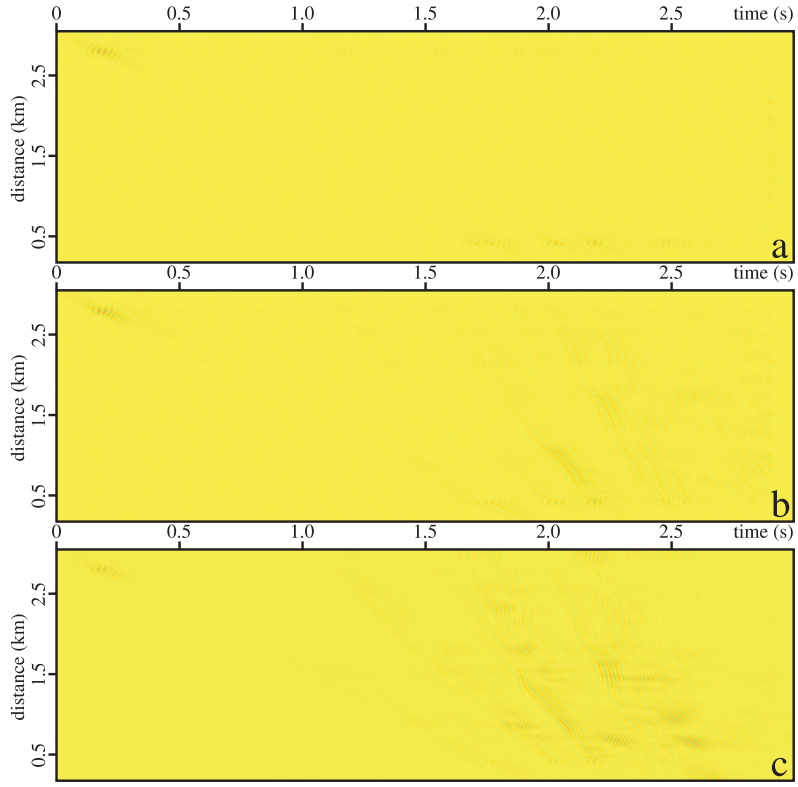

Fig. 4. Differences between the original common shot gather $f(x, t)$ and the approximated common shot gathers $\widetilde{f}(x,t)$ for **(a)** uniform Gaussian packets with $\mathrm{Re}(N_0) = 0.25 \times 10^{-6}$ sm^{-2} and $\mathrm{Im}(N_0) = 0.25 \times 10^{-6}$ sm^{-2}; **(b)** Gaussian packets with $\mathrm{Re}(N) = 0.25 \times 10^{-6}$ sm^{-2} and $\mathrm{Im}(N)$ ranging from 0.125×10^{-6} sm^{-2} to 0.5×10^{-6} sm^{-2}; **(c)** Gaussian packets with $\mathrm{Re}(N) = 0.25 \times 10^{-6}$ sm^{-2} and $\mathrm{Im}(N)$ ranging from 0.75×10^{-7} sm^{-2} to 0.1×10^{-5} sm^{-2}.

Acknowledgements: The author is greatly indebted to L. Klimeš for guidance throughout the work on this topic. The research has been supported by the Grant Agency of the Czech Republic under Contract 205/04/1104, by the Grant Agency of the Charles University under Contract 375/2004/B-GEO/MFF, and by the members of the consortium "Seismic Waves in Complex 3-D Structures" (see \http://sw3d.mff.cuni.cz).

References

Babich V.M. and Ulin V.V., 1981. Complex space time ray method and 'quasiphotons'. *Zapiski Nauchnykh Seminarov Leningradskogo Otdeleniya Matematicheskogo Instituta*, **117**, 5–12 (in Russian; English translation: *Journal of Soviet Mathematics*, **24**, 269–273, 1984).

Daubechies I., 1992. Ten lectures on wavelets. *CBMS-NSF Regional Conference Series in Applied Mathematics*, **61**, SIAM.

Foster D.J. and Huang J.-I., 1991. Global asymptotic solutions of the wave equation. *Geophys. J. Inter.*, **105**, 163–171.

Klauder J.R., 1987. Semiclassical quantization of classically chaotic systems. *Phys. Rev. Lett.*, **59**, 748–750.

Klimeš L., 1986. Discretization error for the superposition of Gaussian beams. *Geophys. J. R. Astron. Soc.*, **86**, 531–551.

Klimeš L., 1989a. Gaussian packets in the computation of seismic wave fields. *Geophys. J. Inter.*, **99**, 421–433.

Klimeš L., 1989b. Optimization of the shape of Gaussian beams of a fixed length. *Stud. Geophys. Geod.*, **33**, 146–163.

Klimeš L., 2004. Gaussian packets in smooth isotropic media. In: *Seismic Waves in Complex 3-D Structures, Report 14*, Dep. Geophys., Charles Univ., Prague, Czech Republic, 43–54, online at "http://sw3d.mff.cuni.cz".

Ralston J., 1983. Gaussian beams and the propagation of singularities. *MAA Studies in Mathematics*, **23**, 206–248.

Thomson C.J., 2001. Seismic coherent states and ray geometrical spreading. *Geophys. J. Inter.*, **144**, 320–342.

Versteeg R.J. and Grau G. (Eds.), 1991. *The Marmousi Experience*. Proc. EAGE workshop on Practical Aspects of Seismic Data Inversion (Copenhagen, 1990), Eur. Assoc. Explor. Geophysicists, Zeist.

Žáček K., 2001. Optimization of the shape of Gaussian beams. *Soc. Expl. Geophys*. *Expanded Abstracts*, **20**, 2128–2131.

Žáček K., 2002. Smoothing the Marmousi model. *Pure Appl. Geophys.*, **159**, 1507–1526.

Žáček K., 2003. Decomposition of the wave field into optimized Gaussian packets. *Soc. Expl. Geophys*. *Expanded Abstracts*, **22**, 1869–1872.

Žáček K., 2004. Gaussian packet pre-stack depth migration. *Soc. Expl. Geophys*. *Expanded Abstracts*, **23**, 957–960.

Žáček K., 2005. Gaussian packet prestack depth migration. *Seismic Waves in Complex 3-D Structures, Report 15*, Dep. Geophys., Charles Univ., Prague, Czech Republic, 29–48, online at "http://sw3d.mff.cuni.cz".

Žáček K., 2006. Optimization of the shape of Gaussian beams. *Stud. Geophys. Geod.*, **50**, 349–366.